SPECTROSCOPIC OBSERVATIONS OF ARCS IN CURRENT LIMITING FUSE THROUGH SAND

T. Chikata* Y. Ueda** Y. Murai** T. Miyamoto**

Mitsubishi Electric Corporation

ABSTRACT Time-resolved spectroscopic observations have been made on arc in current limiting fuse with a silver element. The Ag I, Si I, II, and III lines have been observed successfully through quartz sand in pyrex tube.

As the result, it is suggested that the arc space in the fuse is composed mainly of Si_2O_2 vapour. All of these lines appear simultaneously at the onset of arcing. Their intensities attain to the peaks within 1 μsec. Thereafter, the intensities of the Ag I and Si I lines decay rapidly within 10 μsec. While, the Si II and III lines hold high intensities during whole arcing period. The order of electron density and temperature in the arc of Si vapour have been estimated to be 10^{18} cm^{-3} from line-width and 2×10^4 °K from relative intensity ratio, respectively.

INTRODUCTION Current limiting fuse has been applied widely to electrical systems as an economical protective device. Although many works have been reported on the behavior of current limiting fuse, there are few reports concerned with the properties of the arc in the fuse except some theoretical considerations on the behavior of silver vapor in the quartz sand.(1)(2) But the current limiting phenomena of the fuse can not be understood without making clear the physical properties of arc space in the quartz sand. We revealed the fact that the spectroscopic observation of arcs in the fuse is successfully possible through quartz sand in Pyrex tube. This paper describes the results of spectroscopic investigation on arcs in current limiting fuse with a silver element.

EXPERIMENT

Test Circuit The test circuit is shown schematically in Fig. 1. The constants L,C and charging voltage V_o were chosen to be 1.55 mH, 1000 μF and 1.3 kV, respectively. A prospective short circuit current with the crest value of 1 kA and the frequency of 60 Hz was fed to the model fuse by closing the switch S. The voltage and current waveforms of the fuse were observed by an oscilloscope through a differential voltage divider and a coaxial shunt, respectively.

Model Fuse The cross-sectional view of the model fuse and the element are shown in Fig. 2. The barrel is made of Pyrex glass tube with the inner diameter of 15 mm and the length of 100 mm. The silver ribbon element has a single reduced section as shown in Fig. 2. Quartz sand was used as an arc quenching filler around the element. Three kinds of grain size, #32 ∿ 60, #16 ∿ 32, and #10 ∿ 16, were prepared for the experiment.

---

* Sanda Plant, Itami Works, Mitsubishi Electric Corp., Japan.

** Central Research Laboratory, Mitsubishi Electric Corp., Japan.

In addition, the arcing phenomena of the same silver element stretched in air was studied for the comparison with that of the model fuse.

Spectroscopic Observation Arcs in the fuse were observed by making use of a spectrograph (Type GE 100 Shimazu) as shown in Fig. 1. The observations were carried out aiming at the arcing in the reduced section of the silver element. The calibration of wavelength dependence of the spectrograph including the three photomultipliers was done with a NBS standard lamp, and the relative intensity calibrations of the arc spectrum were performed by taking photographs of the spectrum through neutral filters of four different optical densities. The spectroscopic data were obtained by two methods, the time-integrated spectrogram and the time-resolved observation.

The time-integrated spectra were taken on the photographic plates (Kodak 103 aF) covering the wavelength of 3300 ∿ 5600 Å. Fig. 3 shows the intensity of time-integrated spectra as a function of the wavelength obtained by tracing the photographic plates using a microphotometer. Fig. 3 (a), (b) and (c) correspond to the cases of arcing in the quartz sand with the grain size, #32 ∿ 60, #16 ∿ 32 and #10 ∿ 16, respectively. In these cases, only the spectral lines of Ag I, Si I, Si II and Si III were detected as pointed out in the figures. Fig. 3 (d) shows the case of arcing in air. In this case O I, O II, N I, N II lines were detected as well as Ag I lines.

It is interesting to note that the O I and O II lines can not be observed in the case of arcing in quartz sand in spite of the fact that oxygen is contained in the filler as SiO_2. This problem is treated quantitatively in the discussion.

Time-resolved spectroscopic observation was performed on the basis of the results of the time-integrated spectra obtained above. Five spectral lines of Ag I 5209 Å, Si I 3905 Å, Si II 3858 Å, Si II 4130 Å and SiIII 4560Åwere selected from the spectra as typical lines of arc. Three lines, Ag I line and any two of Si I, II, III lines were detected simultaneously by three photomultipliers as the voltage outputs. Figs. 4 and 5 show the temporal changes of intensities of these lines during the short period just after the onset of the arcing, and during the whole arcing period, respectively. From the oscillograms obtained in Figs. 4 and 5, it is clear that all these lines appear simultaneously at the onset of arcing and their intensities attain to the peaks within 1 μsec. Thereafter the Ag I and Si I lines decay rapidly within 10 μsec, while the Si II line holds high intensity during whole arcing period.

DISCUSSION On the assumption of local thermodynamic equilibrium (LTE), the electron temperature, electron density, and mixing ratio of the Si I or S II to Ag I were determined from the data of the relative intensities of the spectral lines, and the composition of the arc space in the fuse and the arc pressure were also calculated using Saha equations, charge-neutral condition and the equation of the state.

The electron temperature was obtained from the relative intensity of the line pair, Si II 4130 Å and Si II 3858 Å, and the result is shown in Fig. 6. As shown in the figure, the electron temperature does not almost change with time, and the order of the electron temperature is about 2×10^4 °K.

By making use of the electron temperature in Fig. 6, the electron density was estimated from the line pair, Si II 4130 Å and Si III 4568 Å. As shown in Fig. 7 the electron density was kept nearly constant in the arc period as well as the case for electron temperature. The electron

density was also estimated from the Stark broadening of the time-integrated spectral lines, Si I 3905 Å, Si II 3858 Å, 4130 Å and 5056 Å in Fig. 3.(3) Table 1 shows the result, and the electron density of the order of 10^{18} cm^{-3} obtained from the Stark broadening agrees with that from the relative intensity.

The mixing ratio of the three atomic species, Si I, II and Ag I, was also calculated from the relative intensities of the line pairs; Si I 3905 Å and Ag I 5209 Å, Si II 4130 Å and Ag I 5209 Å. Fig. 8 shows the results with the waveforms of the discharge current and arc voltage.

From the time-integrated spectra shown in Fig. 3, it is evident that the arc space in the fuse is composed of the atomic species, Ag I, II, III, Si I, II, III and O I, II, III. To determine the densities of these nine kinds of particles, use was made of six Saha equations for the each particle densities of Ag, Si and O, charge-neutral condition, the ratio 1 : 2 of the silicon to oxygen and the ratio 1 : 40 or 1 : 80 of Ag I to Si II obtained in Fig. 8. In the calculation, the advance of ionization limit of each species due to the electron concentration of 10^{18} cm^{-3} was taken into account. Calculated particle densities are shown in Table 2. The arc pressures calculated at the same time attained to about 6 atm and 5 atm corresponding to the ratio 1 : 80 and 1 : 40 for silver to silicon, respectively. From the calculated results, the reason why the spectral line of O I and II was not observed even by photographic plate of high sensitivity is explained as follows.

The intensity ratio of typical O II line, 4490 Å or 4061 Å, and Ag I line 5209 Å was calculated as given in Table 3, by making use of the particle densities in Table 2, the electron temperature 2 x 10^4 °K and the electron density 1 x 10^{18} cm^{-3}. The spectral intensities of O II lines are far lower than those of Ag I or Si II lines, since the excitation energies for most of O II lines are higher than those for Ag or Si lines. None of O I lines in the wavelength region from 3300 to 5600 Å were observed since the excitation levels of these lines disappear due to the reduction of the ionization energy caused by the high electron density of 10^{18} cm^{-3}.

REFERENCES

(1) L. Vermij, "Electrical behavior of fuse elements", Ph. D. Thesis, pp. 86-96, 1969.
(2) H. W. Mikulecky, "Current-limiting fuse with full-range clearing ability", IEEE Trans. Power App. Syst. PAS-84, pp. 1107-1116, 1965.
(3) H. R. Griem, "Plasma spectroscopy", McGraw-Hill, New York, 1964.

Table I. Electron density Ne calculated from half widths of SiI and SiII lines ($Te = 2\times10^4$)

Spectral lines / mesh		SiI	SiII		
		3905 Å	3858 Å	4130 Å	5056 Å
$Ne\ (cm^{-3})$	10~16	1.4×10^{18}	3.8×10^{18}	2.4×10^{18}	1.2×10^{18}
	16~32	2.4×10^{18}	3.8×10^{18}	3.7×10^{18}	1.5×10^{18}
	32~60	1.6×10^{18}	2.5×10^{18}	2.0×10^{18}	7.4×10^{18}

Table 2. Calculated particle density for $Te = 2\times10^4$°K and $Ne = 10^{18} cm^{-3}$

Mixing ratio / Species of particles	Particle density (cm^{-3})	
	$AgI/SiII = 1/40$	$AgI/SiII = 1/80$
Ag I	4.5×10^{15}	3.0×10^{15}
Ag II	1.3×10^{17}	8.6×10^{16}
Ag III	8.1×10^{16}	5.6×10^{16}
O I	9.6×10^{16}	1.3×10^{17}
O II	4.0×10^{17}	5.3×10^{17}
O III	3.0×10^{13}	4.0×10^{13}
Si I	7.0×10^{15}	9.3×10^{15}
Si II	1.8×10^{17}	2.4×10^{17}
Si III	6.3×10^{16}	8.3×10^{16}

Table 3. Calculated relative intensity ratio of spectral lines

Mixing ratio / Species of particle	Relative intensity	
	$AgI/SiII = 1/40$	$AgI/SiII = 1/80$
$\frac{O\ II\ (4490Å)}{AgI\ (5209Å)}$	3.7×10^{-5}	6.3×10^{-5}
$\frac{O\ II\ (4061Å)}{AgI\ (5209Å)}$	2.1×10^{-5}	1.4×10^{-4}
$\frac{Si\ II\ (4130Å)}{AgI\ (5209Å)}$	0.95	1.5×10^{0}

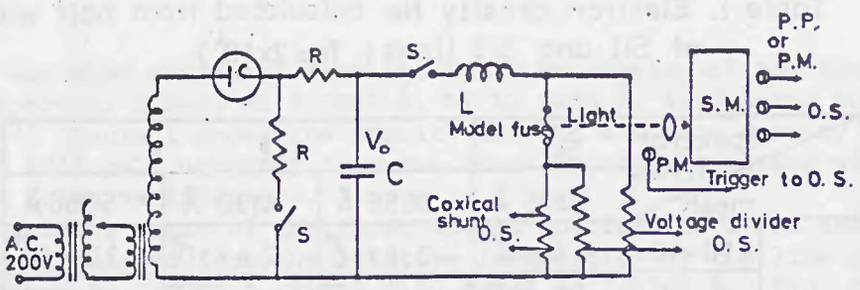

C Capacitance , L Inductance , R Resistance
S Switch , O.S. Oscilloscope , P.M. Photomultiplier
P.P. Photogaphic plate , S.M. Spectrometer

Fig. 1. Schematic of experimental set up

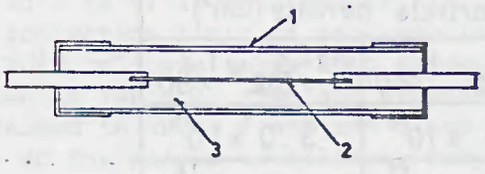

1 Barrel
2 Fuse element
3 Arc quenching filler

Fig.2 Cross-sectional view of model fuse

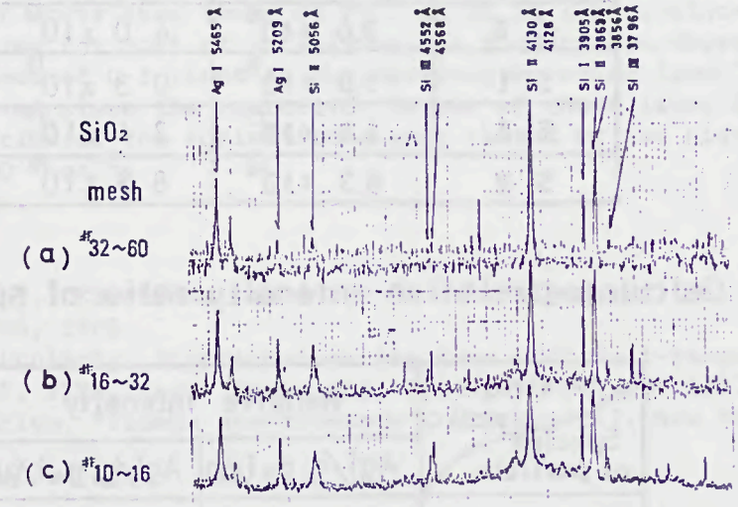

Fig. 3 Time integrated arc spectra in fuses

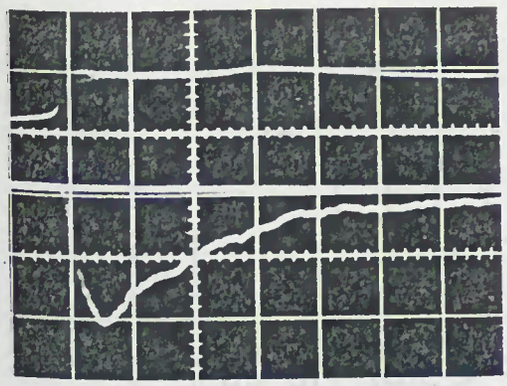

(A) Upper; Arc Voltage
53.4 V/div.
Lower; P.M.(AgI, 5209 A)
0.5 V/div.

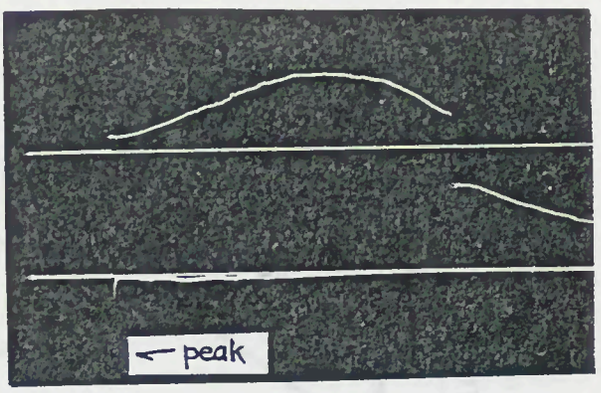

(A) Upper; Arc Voltage
267 V/div.
Lower; P.M. (AgI, 5209 A)
0.5V/div.

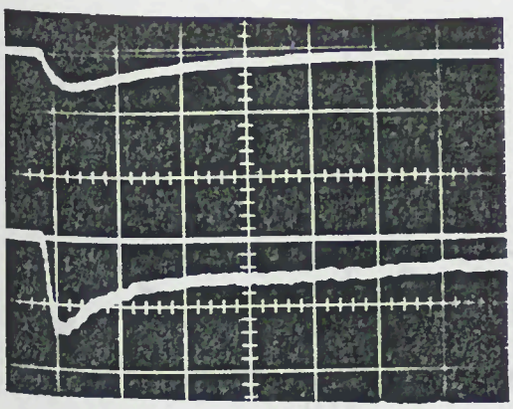

(B) Upper; P.M. (SiI, 3905 A)
0.2 V/div.
Lower; P.M. (SiII, 4130 A)
0.5 V/div.

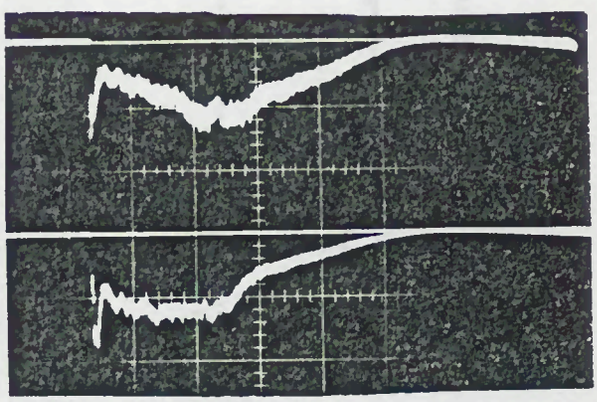

(B) Upper; P.M. (SiI, 3905 A)
0.01 V/div.
Lower; P.M. (SiII, 4130 A)
0.2 V/div.

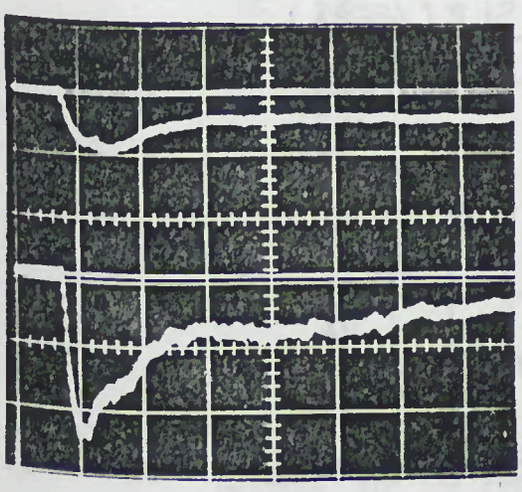

(C) Upper; P.M. (SiII 4130 A)
0.1 V/div.
Lower; P.M. (SiIII, 4560 A)
0.2 V/div.

Fig.4 P.M.output intensity of spectral lines at onset of arcing.(Sweep; 2 μsec/div.)

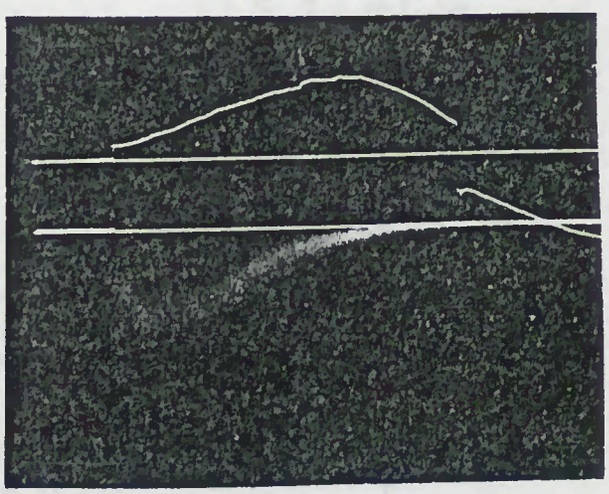

(C) Upper; Arc Voltage
267 V/div.
Lower; P.M. (SiIII,4560 A)
0.05 V/div.

Fig.5 P.M.output intensity of spectral lines during arcing period.
(Sweep; 0.5 msec/div.)

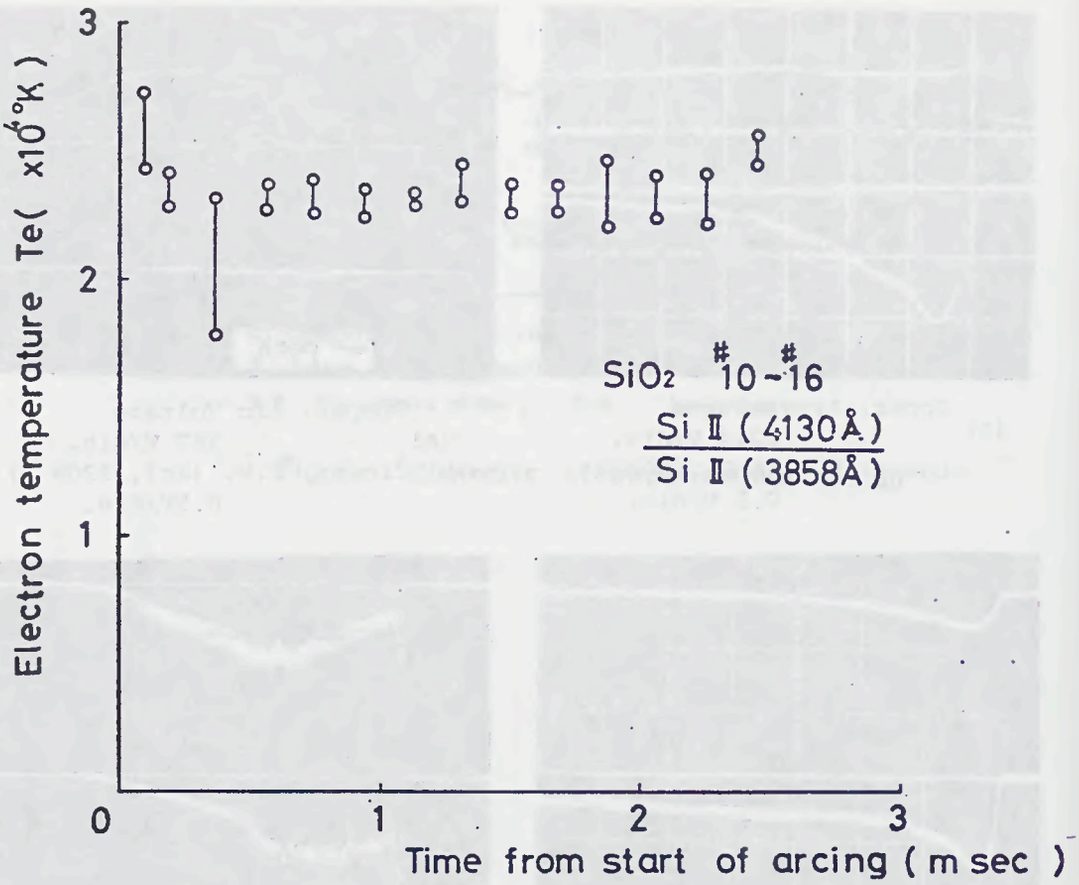

Fig. 6 Values of Te as a function of ta

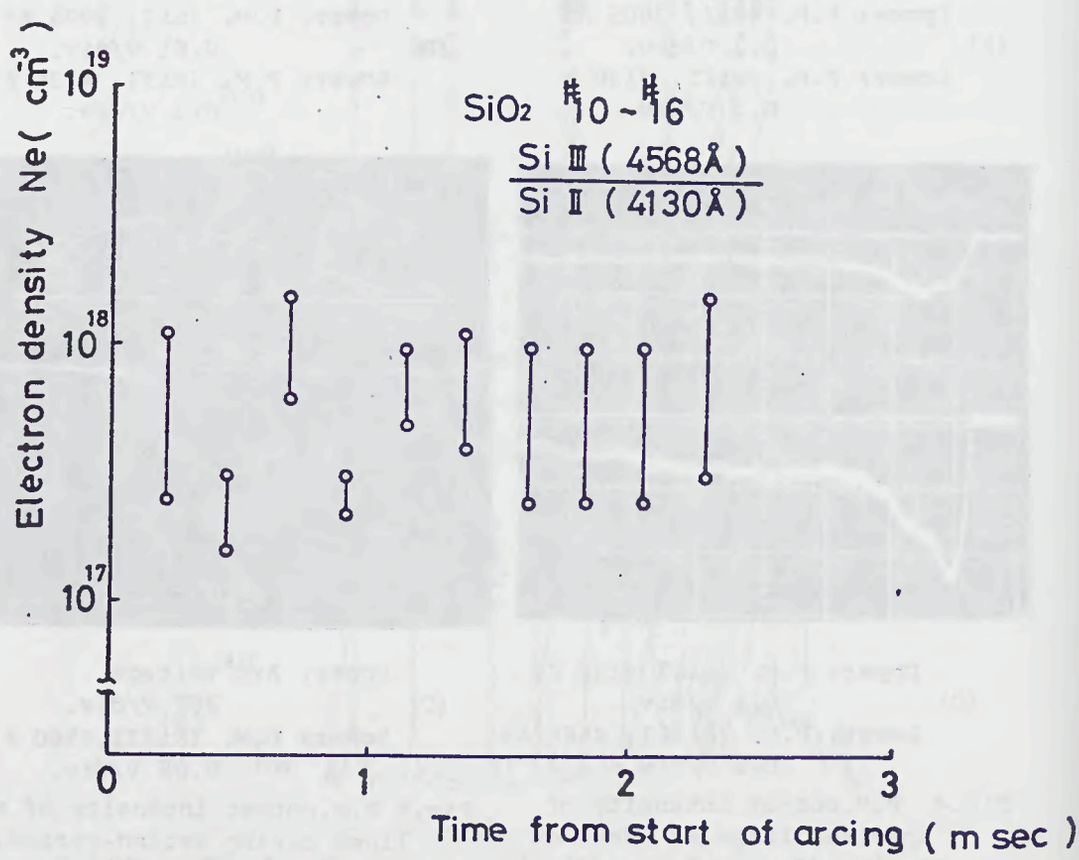

Fig. 7 Values of Ne as a function of ta

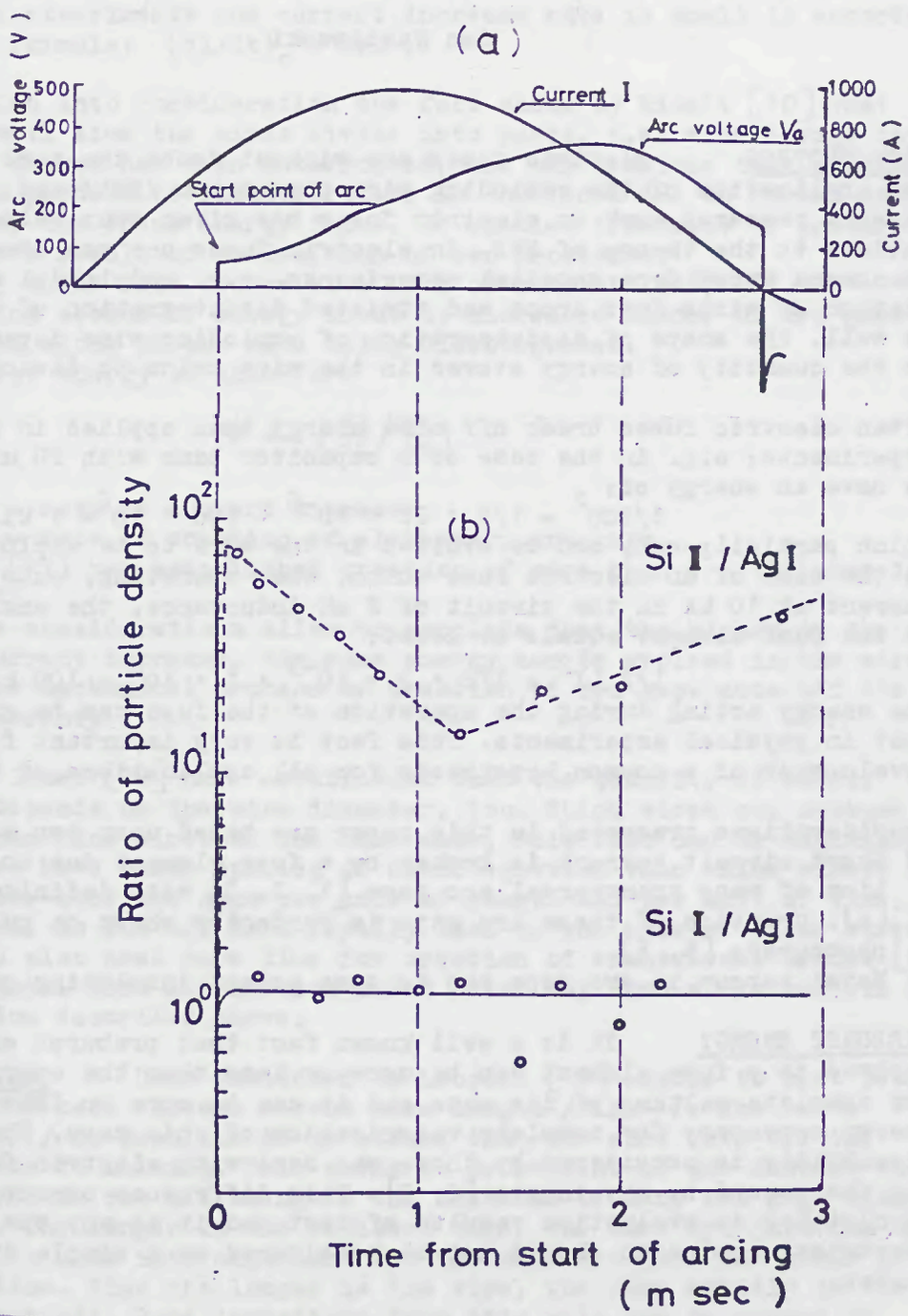

Fig.8 Typical waveforms of the discharge current and arc voltage, and the ratio of silicon to silver.